PREDICTION OF AIR QUALITY CONSIDERING THE CONCEALED AIR LEAKS OF HOUSES

Motoya Hayashi[1], Haruki Osawa[2], Yoshinori Honma[3] and Miyuki Matsui[1]

[1]Department of Living and Cultural Science, Miyagigakuin Women's University, Sendai, Japan
[2] Department of Environment & Fire Research, Building Research Institute, Tsukuba, Japan
[3]Iwate Prefectural University Morioka Junior College, Morioka, Japan

ABSTRACT

In this study, the characteristics of the movement of chemical compounds in the concealed spaces and indoor spaces in houses were investigated using building cut models and a simulation program Fresh2006.

The equivalent leakage areas in the concealed spaces were measured using cut models of wooden structures: a common wooden structure, an improved wooden structure and a wooden (2 inch x 4 inch) stud structure. The movements of chemical compounds were calculated using the measured equivalent leakage areas and the simulation program.

The indoor concentrations of the chemical compounds which volatilized in concealed spaces change with the weather and the behaviors of residents. The infiltration ratios from the concealed spaces to indoor spaces were influenced by mechanical ventilation. The influence of the infiltration upon the indoor air quality was larger in the house with an exhaust ventilation system than with any other ventilation system.

KEYWORDS

Indoor air quality, Air leakage, Ventilation system, Chemical compound, Dynamic calculation

INTRODUCTION

There are many infiltration routes in Japanese traditional wooden houses. The equivalent leakage areas of recent houses have become smaller but the infiltration routes are left in the concealed spaces like beam spaces, crawl spaces and inside-wall spaces. The author's previous studies showed that these routes lead chemical compounds into the indoor spaces from the concealed spaces in test houses. Therefore, the infiltration from concealed spaces was taken into consideration in the amendment of building standard law in 2003. In this study, in order to find an effective method to reduce the infiltration from the concealed spaces, the characteristics of the movement of chemical compounds in the concealed spaces and indoor spaces in houses were investigated using building cut models and a simulation program named Fresh2006.

SIMULATION METHODS

At first, the equivalent leakage areas in the concealed spaces were measured using cut models of wooden

Figure 1 A cut model of an improved post-and-beam wooden structure

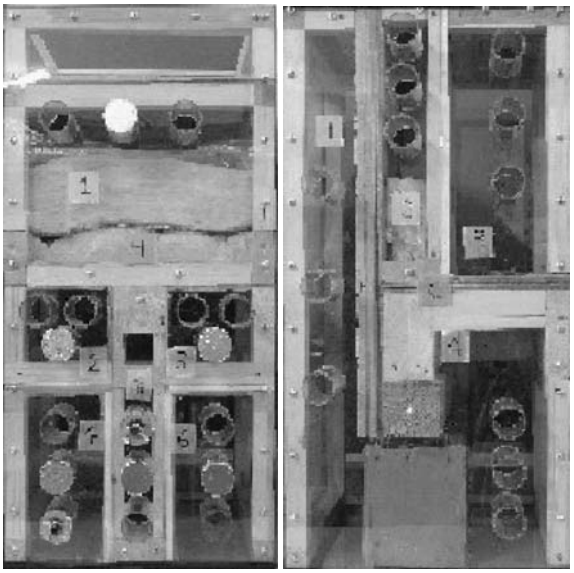

Figure 2 Divided cut models of a wooden (2 inch x 4 inch) stud structure

structures: a common post-and-beam wooden structure, an improved post-and-beam wooden structure built according to the latest building insulation code and a wooden (2 inch x 4 inch) stud structure built according to the latest building insulation code. This code was established in 1999.

It was difficult to measure the equivalent leakage areas in the concealed spaces. So the cut models of these structures were constructed in a laboratory in Miyagigakuin Women's University. Figure 1 shows a cut model of improved post-and-beam wooden structure. The sizes of the elements of the cut model are the same as those of elements of real houses but the height of the cut model was lower than the real houses. A cut model of improved post-and-beam wooden structure built according to the latest insulation code was as the same size. These cut models include several leakages in the concealed spaces of the houses. Cut models of a wooden (2 inch x 4 inch) stud structures were made in another method. Figure 2 shows divided cut models of wooden (2 inch x 4 inch) stud structures. Some partial cut models were made in order to save the space to measurement. These cut models were built by carpenters in the laboratory.

Leakage areas in the concealed spaces and the leakage areas between the concealed spaces and indoor spaces were measured using mass-flow controllers and pressure analyzers. Figure 3 shows the measurement system. When the leakage areas between cell1 and cell2 are measured, cell1 must be opened to the outside and the air pressures of cell3 and cell4 have to be controlled to meet the pressure of cell2. On this condition the air of cell2 goes only to cell1. The airflow rate from cell2 to cell1 accords the air flow rate through the mass-flow controller between the air tank and cell2, so the air flow rate can be known. Figure 4, Figure 5 and Figure 6 show the equivalent leakage areas per 1m of each structure.

Next, the movements of chemical compounds were calculated using the simulation program. The program simulates the temperatures, the air flow rates, the concentrations and the generation rates of pollutants like formaldehyde, carbon dioxide: CO_2 using the NHK standard living schedule model and the HASP weather data on Tokyo.

The simulation program was written in 1996, and was named 'Fresh96'. It was composed of the following three calculation methods.

Dynamic thermal calculation of the temperature, heating and cooling loads: the calculation method was devised by Prof. Aratani: Hokkaido University in 1974. The initial responses of the thermal-flow rates are calculated and the functions of the

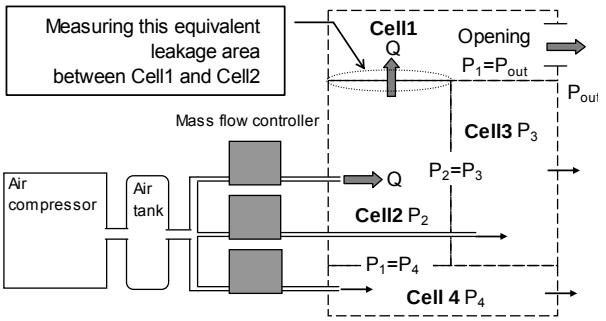

Figure 3 Measurement systems to measure leakage areas between cells

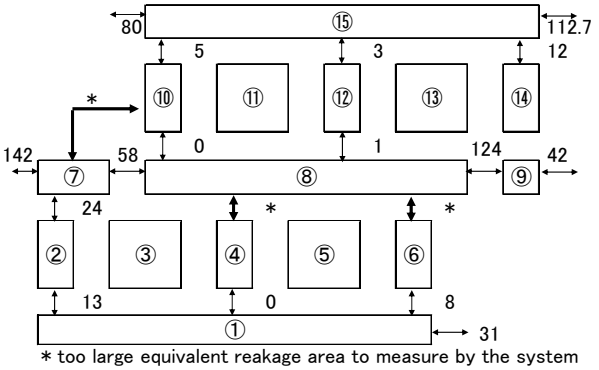

Figure 4 Leakage network of a common post-and-beam structure (cm2/m)

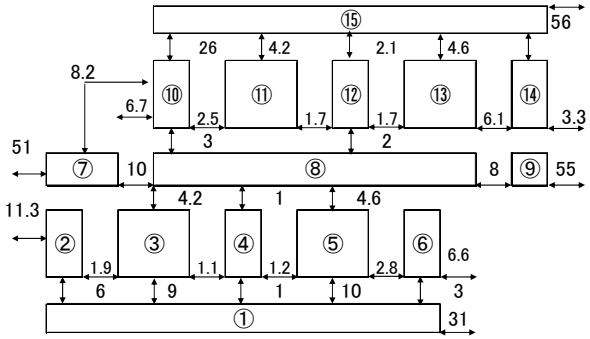

Figure 5 Leakage network of an improved post-and-beam structure (cm2/m)

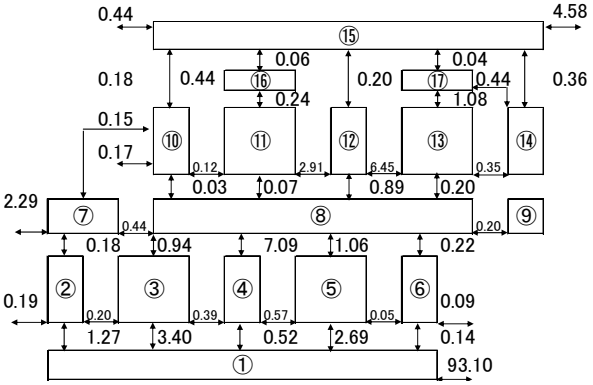

Figure 6 Leakage network of a wooden (2 inch x 4 inch) stud structure (cm2/m)

responses are described as the following equation in order to increase the speed of the calculation.

$$h(t) = B_0 + \Sigma B_m e^{-\beta m \cdot t} + q \cdot \delta(t) \quad \ldots\ldots\ldots\ldots (1)$$

Where, $h(t)$ the initial response of thermal-flow rate, B_0 the steady value of thermal flow rate, $q=\Sigma B_m/\beta_m$ and $\delta(t)$ Delta function.

The temperatures and the heating and cooling loads are calculated with the above equation using Duhamel's integration method. The temperature and the heat loads are calculated using the calculated temperatures in the other rooms and the calculated ventilation rates as the values Δt before. In the following case studies, the interval time Δt was decided to be 5 minutes. The values are calculated using the standard weather data from Society of Heating, Air-conditioning and Sanitary Engineers of Japan and the rates of solar radiation through the windows are calculated considering the effect of shades. The thermal loads by the human behaviors such as cooking, watching television and cleaning rooms, are calculated from the daily schedule model of a family. The air-conditioner and the windows are operated to make the indoor climate comfortable considering the daily schedule of a family. The air-conditioning systems and the windows are controlled as follows: The room temperatures are controlled to be above 22deg.C with a central heating system. The room temperatures are controlled to be above 22deg.C and below 28deg.C by opening windows in houses with a central heating system. The room temperatures are controlled to be below 28deg.C by cooling the rooms.

Calculation of air flow rate in the multi-cell system using the equation of the power at the openings: the airflow rates are calculated using the following equations which are led by the balances of power at openings.

$$[D] \cdot \{q^n\} + [K] \{\int qdt\} = \{F_{wind}\} + \{F_{temp}\} + \{F_{fan}\} \ldots (2)$$

where q *the* airflow rate, n the exponent of airflow friction, $[D]$ the matrix of airflow friction, $[K]$ the matrix of room air elasticity, $\{F_{wind}\}$ the power of wind, $\{F_{temp}\}$ the power by the room air density $\{F_{fan}\}$ the power of fan.

The equations can be solved using Newmark's numerical integration method. The ventilation rates are calculated considering the stack effect, the wind pressure and the mechanical power using the standard weather data, the ratios of the wind pressure, the ratio of wind speed considering the circumstances and the performance of the fans. In the case of the following studies, the ratio of wind speed at the town to the speed at the plain flat ground was 0.4.

Dynamic calculation of concentrations of pollutants using the equation of the amount of pollutants: the

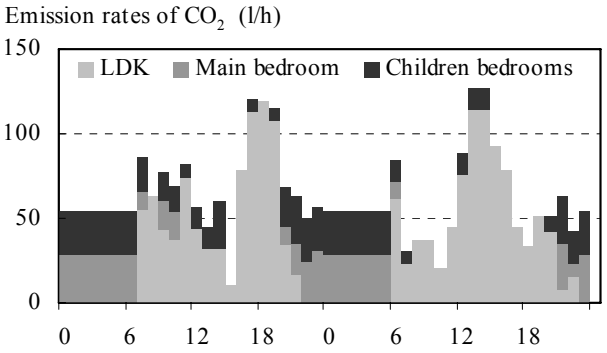

Figure 7 Calculated emission rates of CO_2

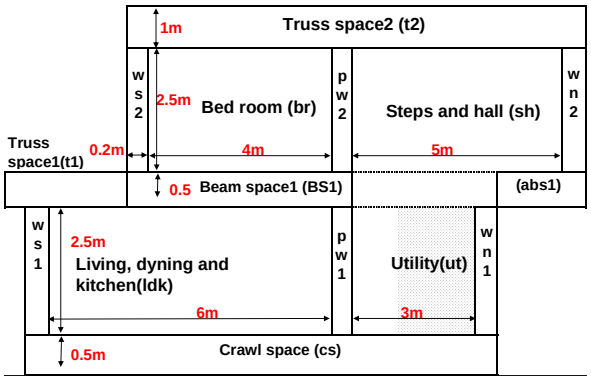

Figure 8 Building model for simulations

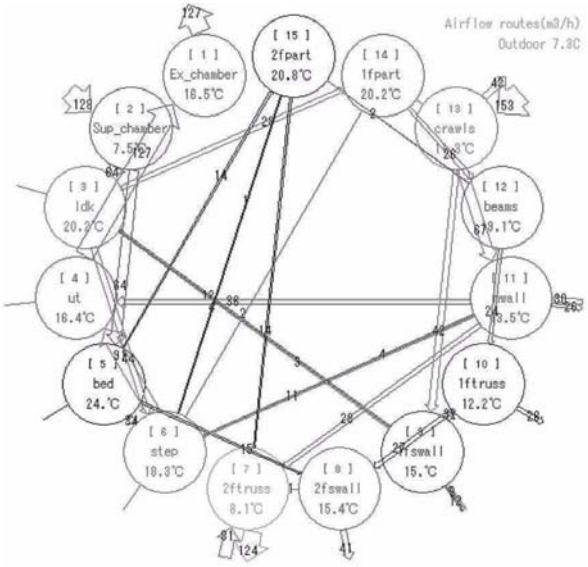

Figure 9 Window of Fresh2006 during calculation

concentrations of pollutants in each room are calculated using the following equations which are led by the balance of the volume of the pollutants.

$$[Q] \cdot \{C(t)\} + [V] \cdot \{C'(t)\} = \{M(t)\} \ldots\ldots\ldots\ldots (3)$$

where $[Q]$ the matrix of airflow rate $Q(i,j)$: the airflow rate from room-i to room-j, $Q(k,k)$= -

$\Sigma_{k<>i}Q(k,i)$, *C(t)* the concentration of a pollutant, *[V]* the volume of rooms, *{M}* the emission rates of a pollutant in each room.

The equations can be solved using Newmark's numerical integration method. The emission rates of CO_2 are calculated using the average Japanese daily schedule and the data on the emission rates caused by the people's behavior in houses shown in Table1. The daily schedule of each family in a house is calculated considering the plan of the house using the results of the survey on the Japanese daily schedule by NHK. Figure 7 shows the calculated emission rates of CO_2 on a holiday and a weekday in the house model. The emission rates of CO_2 change with the behavior of the family and the emission rates are high in the bedrooms on the second floor at night and the emission rates are high in the living room on the first floor at daytime. This is the pattern of emission rate of CO_2 in a general Japanese detached house.

The emission rates of formaldehyde were calculated using an equation. The influences of temperature and sink were considered in the equation.

$$E = E25 \cdot a^{(T-25)} - \beta \cdot C(t) \quad \text{.....(4)}$$

Where E: emission rate ($\mu g/h.m^2$), E_{25} (=100 $\mu g/h.m^2$): emission rate measured in small chamber when temperature is 25deg.C, T: temperature, a=1.11: measured in small chamber, β (= 0.06): ratio of sink measured in small chamber, C(t): concentration ($\mu g/m^3$)

In these studies, in order to make clear the influence of the infiltration of chemical compounds from beam spaces and a crawl space to indoor space upon the indoor air quality, SF6 was released at the beam spaces and R22 was released at the crawl space in the simulation models shown in Figure 8. Formaldehyde emission rates in the concealed spaces are set to be $100\mu g/h.m^2$ considering the surface area of emission sources like plywood and the emission rates. This model was designed considering the shape of a low house with two stories. The emission rates of SF6 and R22 were 300ml/h. The movement and the concentrations of each gas were calculated. The outdoor concentrations were set as follows. The concentration of carbon dioxide: CO_2 is 400ppm, that of formaldehyde 0$\mu g/m^3$, that of SF6 0ppm and that of R22 0ppm. Figure 9 shows a window of "Fresh2006" which is the latest version of "Fresh" during the calculation.

RESULTS

At first, the equivalent leakage areas of the three structures were measured using this simulation program. A large fan was set and the inside air was exhausted. The airflow rates are controlled to meet five ranks of airflow rate and the pressure differences were calculated. The equivalent leakage areas were calculated. The equivalent leakage area of the model with a common wooden structure was $5.0cm^2/m^2$, that of an improved structure was $2.8cm^2/m^2$ and that of a wooden (2inch x 4inch) stud structure was $0.3cm^2/m^2$.

Figure 10 and Figure 11 show the hourly change of formaldehyde concentrations in winter. The concentrations in the beam space (bs1) in the case of exhaust and supply ventilation in Figure 11 is higher than those in the case of exhaust ventilation in Figure 10. The formaldehyde stays longer in the beam space in the case of an exhaust and supply ventilation. But the indoor concentrations are lower in the case of exhaust and supply ventilation. These results show that the influences of the concealed spaces upon the indoor air concentrations depend on the ventilation method.

Figure 12 and figure 13 show the airflows in a common structure. In the case of exhaust ventilation

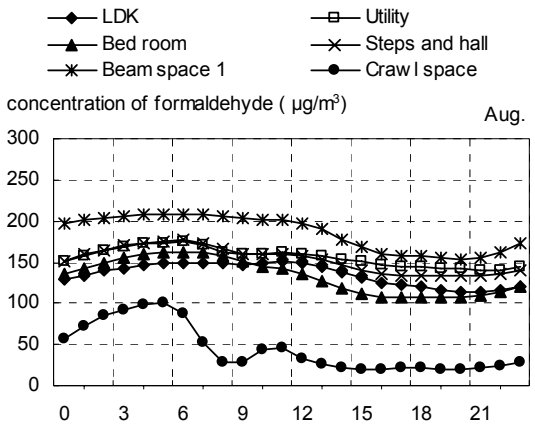

Figure 10 Hourly change of formaldehyde in a house with an improved structure and an exhaust ventilation system

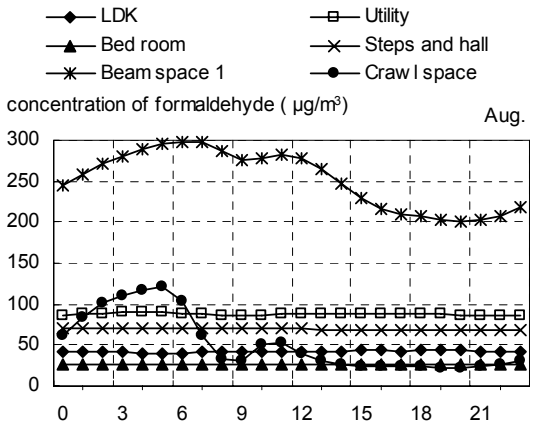

Figure 11 Hourly change of formaldehyde in a house with an improved structure and an exhaust-and-supply ventilation system

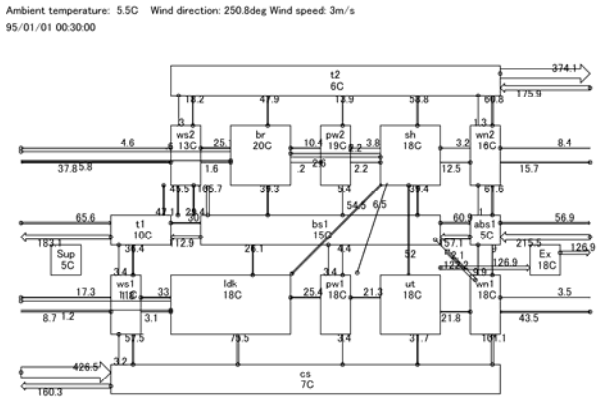

Figure 12 Calculated airflow rates in a common structure with an exhaust ventilation system

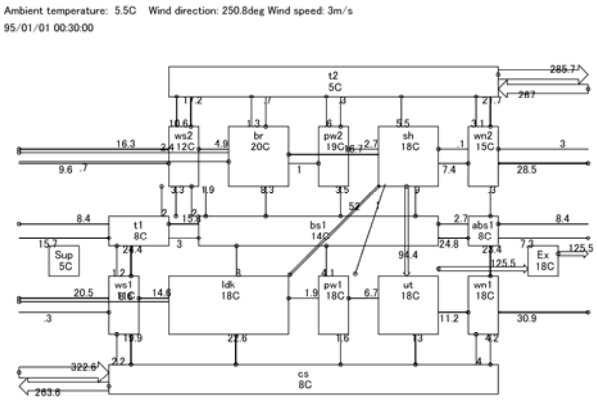

Figure 14 Calculated airflow rates in an improved structure with an exhaust ventilation system

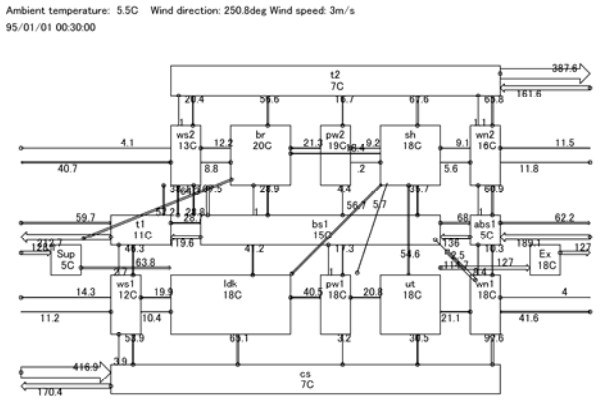

Figure 13 Calculated airflow rates in a common structure with an exhaust and supply ventilation system

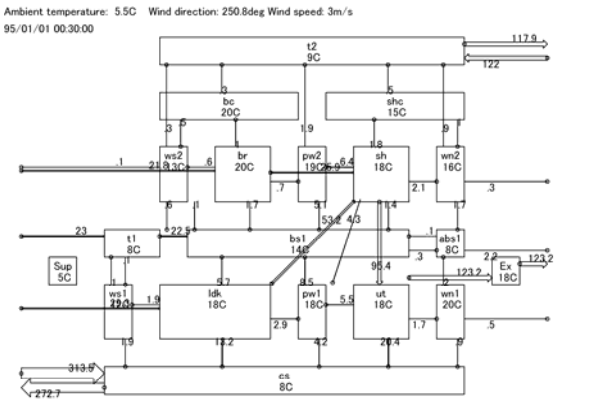

Figure 15 Calculated airflow rates in a wooden (2 inch x 4 inch) structure with an exhaust ventilation system

in figure 12, the air goes from concealed spaces to indoor spaces. The air goes from the crawl space to the indoor space on the second floor through the wall and truss space (t1). Several routes from concealed spaces to indoor spaces are shown in these figures. In the case of exhaust and supply ventilation in figure13, these routes are also recognized.

Figure 14 and figure 15 show the airflow in the case of exhaust ventilation. The airflow rates through the above routes became lower in these airtight structures: an improved structure and a wooden (2 inch x 4 inch) stud structure. The airflow rates through these routes become very low in the cases of airtight structures.

Figure 16 shows the annual change of temperature difference and wind speed in Tokyo. Figure 17 shows the calculated airflow rates directly from the outside to indoor spaces. In mild seasons like June and September, some airflow rates became higher than in winter, because the windows were opened to make indoor climate comfortable. In mid-summer, the indoor spaces were cooled by air conditioner and

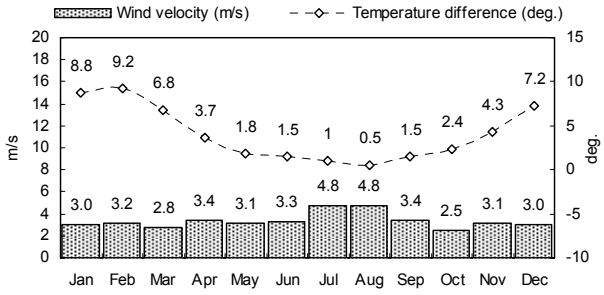

Figure 16 Annual change of temperature difference and wind speed

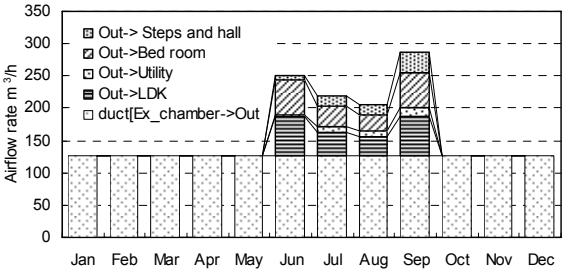

Figure 17 Airflow rates in an improved structure with an exhaust and supply ventilation system

these airflow rates became lower than those in mild seasons.

Figure 18 shows the annual change of calculated concentrations. These concentrations are monthly averages. The concentrations of carbon dioxide were steady and low. The concentrations in the bed room (br) were the highest because the air supply through the ventilator was not high enough. These characteristics were shown in common structures with many air leaks. The annual change of formaldehyde concentrations shows interesting characteristics. Generally, the concentrations decrease but the concentrations were high in summer except for the concentrations in bedroom that were high in the early months. These characteristics were based on the following mechanisms. The emission rate of formaldehyde increases with temperature. The emission ability declines with the integral volume of emission.

SF6 is released in the beam space (bs1). The concentrations of SF6 are low in summer and the concentrations in the bed room (br) are higher than those in the other spaces. In winter, the air supply to bed room is not high enough due to the large temperature difference but it becomes sufficient in mild seasons and summer. In the mild seasons the windows were opened. These change of conditions influenced the change of concentrations.

R22 is released in the crawl spaces (cs). The concentrations of R22 are lower than SF6 concentrations. The crawl spaces are connected to the outside through openings according to the building code to keep wooden structures. But the indoor concentrations are not zero. This result shows that it is necessary to keep the emission rates of chemical compounds like organic phosphorus insecticide low even in the crawl space.

Figure 19 shows the infiltration ratios from beam space to indoor space. The infiltration ratio accords to a ratio of the infiltration rate of gas to indoor spaces toward the emission rate in concealed spaces. The ratios are high in the cases of exhaust ventilation system and airtight structures. In these cases, indoor spaces are decompressed and pollutants are pulled inside from the concealed spaces. Therefore when the windows are opened, the ratios become lower. In the case of crawl spaces, the ratios are lower than those in the case of beam space.

Figure 20 shows the comparison of concentrations. In the case of carbon dioxide, the concentrations are higher with an exhaust ventilation system and an airtight structure. This tendency is much stronger in the case of formaldehyde, SF6 and R22 than in the case of carbon dioxide.

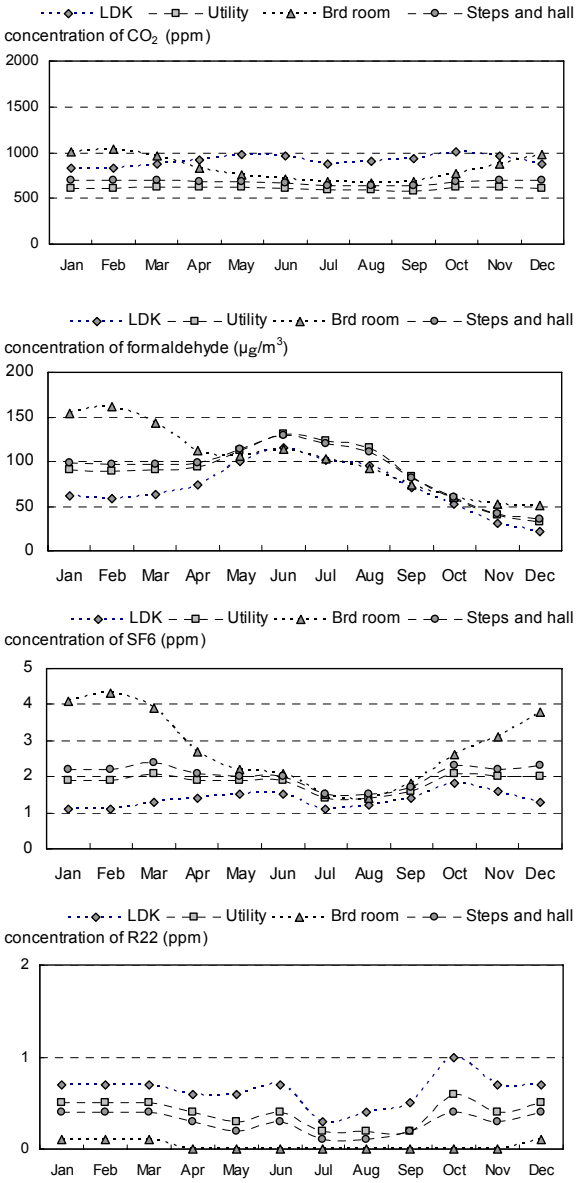

Figure 18 Calculated concentrations in an improved structure with an exhaust ventilation system

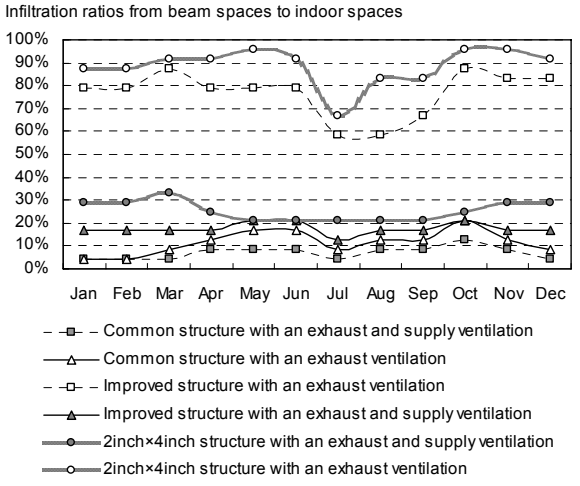

Figure 19 Annual changes of infiltration ratios from the concealed spaces to indoor spaces

Figure 21 shows the infiltration ratios from concealed spaces to indoor spaces. The figure shows the above-mentioned tendency too and shows that it is necessary to design ventilation routes considering the air leaks and the emission of pollutants in the concealed spaces for better indoor air quality.

Lastly, the calculated infiltration ratios are compared

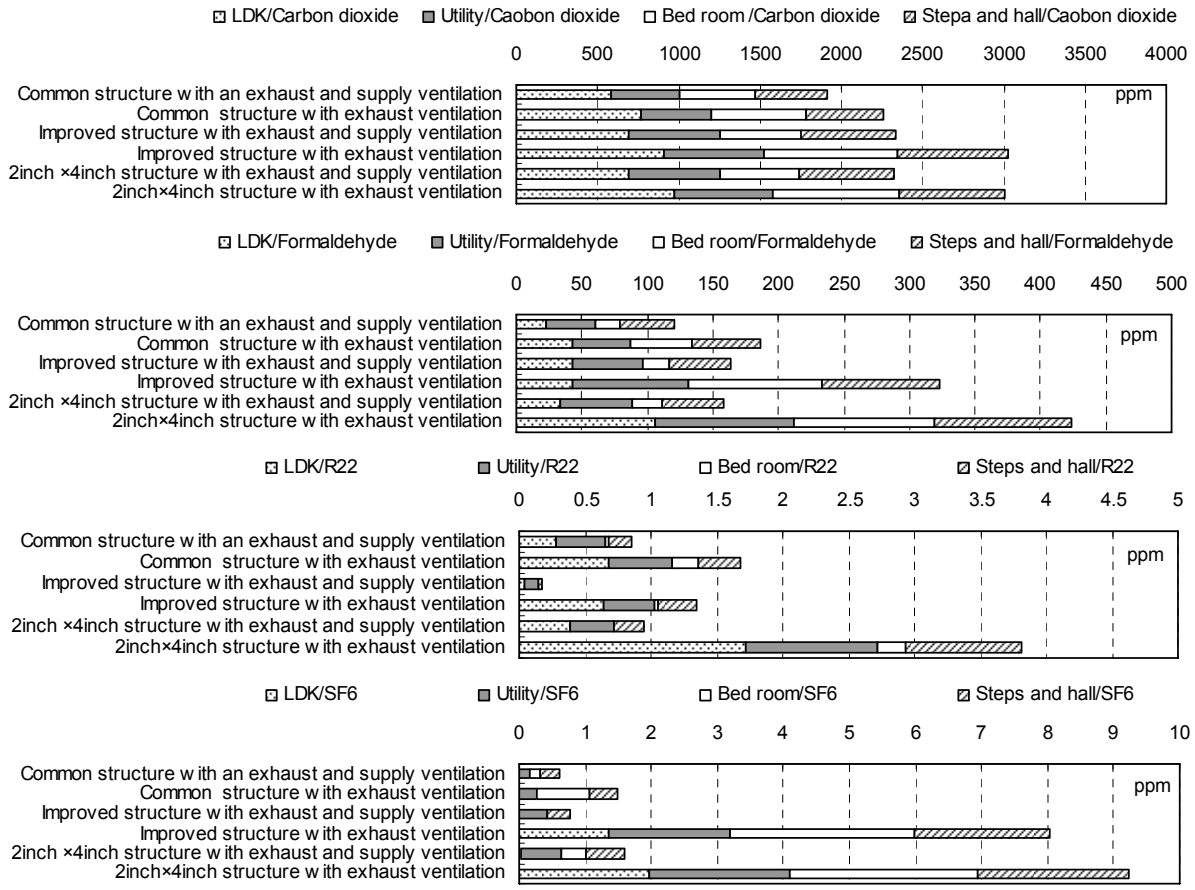

Figure 20 Calculated indoor concentrations of each case study

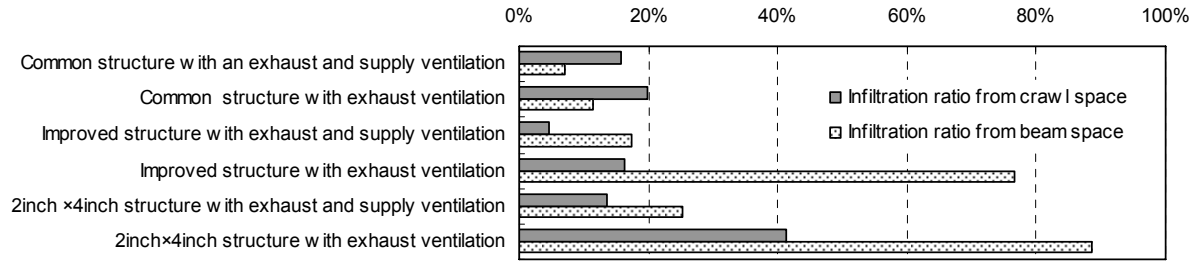

Figure 21 Infiltration ratios from the concealed spaces to indoor spaces in each case study

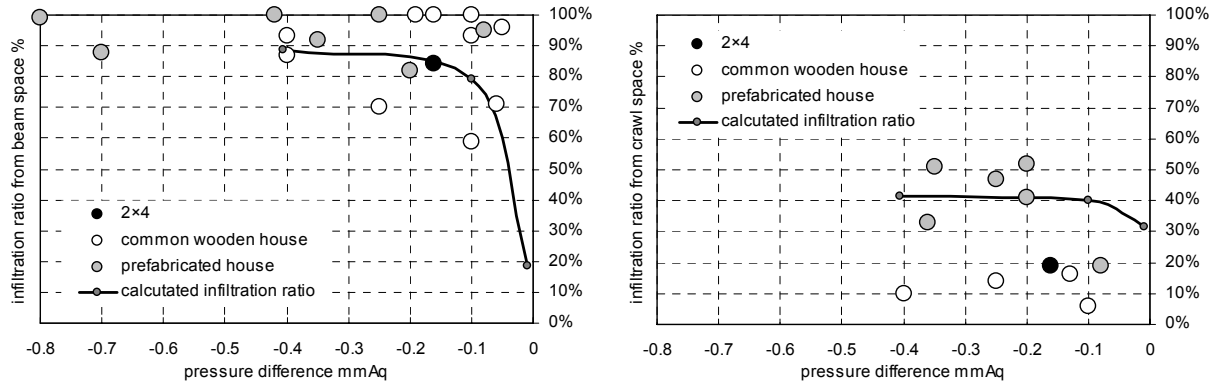

Figure 22 Comparison between the calculated infiltration ratios and the measured ratios in real houses

with the measured ratios in real houses: common wooden houses, prefabricated houses and a wooden (2 inch x 4 inch) stud houses as shown in Figure 22. The ratios are measured using tracer gases: SF6 and R22. The tracer gases are released constantly in the concealed spaces and in the indoor spaces and the concentrations were measured indoors. The ratios were calculated from the concentrations and the emission rates.

The calculated infiltration ratio from beam space increases with the decompression level. The calculated ratio in the case of a wooden (2 inch x 4 inch) stud structure is the highest and the level of decompression is also the highest. In the case of a common structure, the calculated ratio and the decompression level are both the lowest. The measured ratios have the same tendency. In the case of the ratio from crawl spaces, the measured ratios are lower but the above-mentioned tendency remains.

CONCLUSIONS

The concealed infiltration routes were shown for the first time by the measurements of equivalent leakage areas using cut models of Japanese houses and the simulation considering the weather and Japanese living habit. The indoor concentrations of the chemical compounds which volatilized in concealed spaces changed with the weather and the behaviors of the residents. The infiltration ratios from the concealed spaces to indoor spaces were influenced by mechanical ventilation. The influence of the infiltration upon the indoor air quality was larger in the house with an exhaust ventilation system than with any other ventilation system. These results show that it is necessary to consider the materials and the leakages in the concealed spaces for a countermeasure against sick house syndrome especially in the case of exhaust ventilation. The results will show the design guide line for designing better indoor air quality effectively.

ACKNOWLEDGEMENTS

The study was a part of a national project "Development of Countermeasure Technology on Residential Indoor Air Quality" by National Institute for Land and Infrastructure Management under the Japanese government. The study was carried out by Grant-in-Aid Scientific Research of Japan Society for the Promotion of Science. The investigations were made with the cooperation of Center for Housing Renovation and Dispute Settlement Support, The Center for Better Living and the students of Miyagigakuin Women's University. The authors express their gratitude to Dr.NoboruAratani, Prof. MasamichiEnai, Prof. HiroshiYoshino, Dr. TakaoSawachi, and Prof. AtsuoNozaki.

REFERENCES

NHK. 1990. "The survey on the Japanese daily schedule 1990"

M.Hayashi and H.Yamada 1996. "Performance of a passive ventilation system using beam space as a fresh_air supply chamber, Proc. of INDOOR AIR '96 Vol.1 859-864 JULY 21-261.

M.Hayashi, M.Enai and Y.Hirokawa, 2001. "Annual characteristics of ventilation and indoor air quality in detached houses using a simulation method with Japanese daily schedule model", The International Journal of Building Science and its Applications 'BUILDING AND ENVIRONMENT' Vol.36, No.6 July 2001,721-731

M.Hayashi and H.Osawa, 2005. "The influence of the concealed pollution sources upon the indoor air quality in houses", Proc. of INDOOR AIR '05 ", Paper ID: 2.7-30,2005/9

Hiroshi Yoshino, Kentaro Amano, Mari Matsumoto, Koji Netsu, Koichi Ikeda, Atsuo Nozaki, Kazuhiko Kakuta, Sachiko Hojo and Satoshi Ishikawa, 2004. Long-Termed Field Survey of Indoor Air Quality and Health Hazards in Sick House, Journal of Asian Architecture and Building Engineering, Vol. 3 (2004) No. 2 pp.297-303

Rika Funaki and Shin-ichi Tanabe, 2002. Chemical Emission Rates from Building Materials Measured by a Small Chamber, Journal of Asian Architecture and Building Engineering, Vol. 1 (2002) No. 2 pp.2_93-100

NOMENCLATURE

B_0: the steady value of thermal-flow rate

$C(t)$: the concentration of a pollutant

$[D]$: the matrix of airflow friction

$\{F_{temp}\}$: the power by the room air density

$\{F_{wind}\}$: the power of wind

$h(t)$: the initial response of thermal-flow rate

$[K]$: the matrix of room air elasticity

$\{M\}$: the emission rate of a pollutant in each room.

n: the exponent of airflow friction

q : the airflow rate

$[Q]$: the matrix of airflow rate

$Q(i,j)$: the airflow rate from room-i to room-j

$[V]$: the volume of a room

$\delta(t)$: Delta function